Electronic Supplementary Information

Bisulfate as a Redox-active Ligand in Vanadium-based Electrocatalysis for CH_4 Functionalization

Danlei Xiang,‡[a] Sheng-Chih Lin,‡[b] Jiao Deng,[a] Hao Ming Chen*[b] and Chong Liu*[ac]

[a] Department of Chemistry and Biochemistry, University of California Los Angeles, Los Angeles, California 90095, United States.

E-mail: chongliu@chem.ucla.edu

[b] Department of Chemistry, National Taiwan University, Taipei 10617, Taiwan.

E-mail: haomingchen@ntu.edu.tw

[c] California NanoSystems Institute, University of California Los Angeles, Los Angeles, California 90095, United States.

* Corresponding authors.

‡ Danlei Xiang and Sheng-Chih Lin have equally contributed to this work.

Index *Page*

Materials and methods

Supplementary Figures

Supplementary Tables

Materials and Methods

Chemicals and materials. All reagents were used without further purification unless otherwise specified and were obtained from Sigma-Aldrich, Inc., Thermo Fisher Scientific, Inc., or VWR International, LLC. Dimethyl sulfoxide-d$_6$ (D, 99.9%) was attained from Cambridge Isotope Laboratories, Inc. Deionized (DI) water (18 MΩ cm^{-1} resistivity) was produced from the Milli-Q Water Purification System of Millipore. Fluorine-Tin-Oxide (FTO) Coated Glass Plates (TEC7) were purchased from Hartford Glass, Inc. Chemically pure (CP) grade CH_4 (Min. Purity 99.5%) and ultra high pure (UHP) grade N_2 (Min. Purity 99.999%) were supplied by Airgas, Inc.

Chemical characterizations. Ultraviolet-Visible (UV-Vis) spectra were processed through Agilent/HP 8453 UV-Visible Spectrophotometer. ^{1}H NMR spectra were recorded on Bruker Avance spectrometer (400 MHz). X-ray Absorption Near Edge Structure (XANES) and Extended X-ray Absorption Fine Structure (EXAFS) were recorded at BL17C of National Synchrotron Radiation Research Center (NSRRC), Hsinchu, Taiwan.

Catalyst preparation. Electrolytes with different concentration ratios (c_{H3PO4} (M)/c_{H2SO4} (M)) were obtained by mixing concentrated H_2SO_4 (98%) and crystalline H_3PO_4 (≥ 99.0%) based on their densities. Seven ratios were utilized in this work including c_{H3PO4}/c_{H2SO4} = 0/18.0, 1.2/16.9, 2.3/15.8, 3.5/14.6, 4.7/13.5, 5.8/12.4, and 7.0/11.3. Complex **1**, serving as a homogeneous catalyst in the electrolyte of c_{H3PO4}/c_{H2SO4} = 0/18.0, was prepared by dissolving vanadium pentoxide (V_2O_5) in concentrated H_2SO_4 (98%) with 6 h ultra-sonication. Complex **2**, serving as a precatalyst in liquid phase, coexisted with **1** after dissolving vanadium pentoxide (V_2O_5) in the mixed H_3PO_4-H_2SO_4 electrolytes (c_{H3PO4}/c_{H2SO4} = 1.2/16.9, 2.3/15.8, 3.5/14.6, 4.7/13.5, 5.8/12.4, and 7.0/11.3) with 8 h ultra-sonication.

Data analysis of UV-Vis results. Two vanadium species are involved in the binary H_3PO_4-H_2SO_4 electrolytes since we observed the existence of an isosbestic point at 309 nm, which is a diagnostic of superposition of the spectra for two substances. One vanadium species (**1**) with known dimer structure is fully coordinated with bisulfate ligand ($-OSO_3H$).[1] The other species (**2**) has an unknown structure, either a dimer or a monomer, and is supposed to be a vanadium complex ligated with both bisulfate ligands ($-OSO_3H$) and phosphate ligands ($-OPO_3H_2$). A chemical equilibrium between **1** and **2** exists, which is proposed to be the ligand substitution. Because of the constant reaction stoichiometry indicated by the existence of isosbestic point,[2,3] here we ruled out the scenario that **2** could be a monomer decomposed from **1** ($V_2{-}OSO_3H + n\ H_3PO_4 \rightarrow 2\ V{-}OPO_3H_2 + n\ H_2SO_4$) and then confirmed that **2** should be a dimer based on the structural information analyzed from UV-Vis spectroscopy and EAXFS. The rigorous exclusion process is not discussed here.

Taking advantage of the well-defined two-species equilibrium informed by the presence of isosbestic point,[2,3] we established a mathematical model to determine the molar compositions of **1** and **2** in Fig. 2b. In a mixed solvent of a specific c_{H3PO4}/c_{H2SO4} value, the absorbances at 329 nm and 291 nm (A_{329}, A_{291}, respectively; C_V = 0.4 mM) depend on the concentrations of **1** and **2** ([**1**] and [**2**], respectively), as well as their molar extinction coefficients at 329 nm and 291 nm ($\varepsilon_{329,\mathbf{1}}$ and $\varepsilon_{291,\mathbf{1}}$ for **1**, $\varepsilon_{329,\mathbf{2}}$ and $\varepsilon_{291,\mathbf{2}}$ for **2**, respectively),

$$\frac{A_{329}}{C_V} = \varepsilon_{329,\mathbf{1}} \frac{[\mathbf{1}]}{[\mathbf{1}] + [\mathbf{2}]} + \varepsilon_{329,\mathbf{2}} \frac{[\mathbf{2}]}{[\mathbf{1}] + [\mathbf{2}]} \qquad (1)$$

$$\frac{A_{291}}{C_V} = \varepsilon_{291,\mathbf{1}} \frac{[\mathbf{1}]}{[\mathbf{1}] + [\mathbf{2}]} + \varepsilon_{291,\mathbf{2}} \frac{[\mathbf{2}]}{[\mathbf{1}] + [\mathbf{2}]} \qquad (2)$$

where the molar composition of **1** ($\frac{[\mathbf{1}]}{[\mathbf{1}]+[\mathbf{2}]}$) can be represented by the atomic percentage of vanadium from **1** (x), and the molar composition of **2** ($\frac{[\mathbf{2}]}{[\mathbf{1}]+[\mathbf{2}]}$) can be represented by the atomic percentage of vanadium from **2** ($1 - x$), $\frac{A_{329}}{C_V}$ and $\frac{A_{291}}{C_V}$ can be simplified as the observed molar extinction coefficients $\varepsilon_{329,\ obs}$ and $\varepsilon_{291,\ obs}$, respectively.

Now, the above relationships can be written as

$$\varepsilon_{329,obs} = \varepsilon_{329,\mathbf{1}} \times x + \varepsilon_{329,\mathbf{2}} \times (1 - x) \qquad (3)$$

$$\varepsilon_{291,obs} = \varepsilon_{291,\mathbf{1}} \times x + \varepsilon_{291,\mathbf{2}} \times (1 - x) \qquad (4)$$

Utilizing the spectra data of vanadium(V) in six H_3PO_4-H_2SO_4 electrolytes (c_{H3PO4}/c_{H2SO4} = 1.2/16.9, 2.3/15.8, 3.5/14.6, 4.7/13.5, 5.8/12.4, and 7.0/11.3), the two sets of equations can be written as twelve equations, generating six x values for each electrolytes composition. The subscripts from 1 to 6 represent each electrolytes composition.

Expanded from eqn (3),

$$\varepsilon_{329,obs,1} = \varepsilon_{329,\mathbf{1}} \times x_1 + \varepsilon_{329,\mathbf{2}} \times (1 - x_1) \qquad (5)$$

$$\varepsilon_{329,obs,2} = \varepsilon_{329,\mathbf{1}} \times x_2 + \varepsilon_{329,\mathbf{2}} \times (1 - x_2) \tag{6}$$

$$\varepsilon_{329,obs,3} = \varepsilon_{329,\mathbf{1}} \times x_3 + \varepsilon_{329,\mathbf{2}} \times (1 - x_3) \tag{7}$$

$$\vdots$$

$$\varepsilon_{329,obs,6} = \varepsilon_{329,\mathbf{1}} \times x_6 + \varepsilon_{329,\mathbf{2}} \times (1 - x_6) \tag{10}$$

Expanded from eqn (4),

$$\varepsilon_{291,obs,1} = \varepsilon_{291,\mathbf{1}} \times x_1 + \varepsilon_{291,\mathbf{2}} \times (1 - x_1) \tag{11}$$

$$\varepsilon_{291,obs,2} = \varepsilon_{291,\mathbf{1}} \times x_2 + \varepsilon_{291,\mathbf{2}} \times (1 - x_2) \tag{12}$$

$$\varepsilon_{291,obs,3} = \varepsilon_{291,\mathbf{1}} \times x_3 + \varepsilon_{291,\mathbf{2}} \times (1 - x_3) \tag{13}$$

$$\vdots$$

$$\varepsilon_{291,obs,6} = \varepsilon_{291,\mathbf{1}} \times x_6 + \varepsilon_{291,\mathbf{2}} \times (1 - x_6) \tag{16}$$

The red terms are the unknown parameters to be solved, the black terms are the known values. $\varepsilon_{329,\mathbf{1}}$ and $\varepsilon_{291,\mathbf{1}}$ were extracted from the spectra of $c_{H3PO4}/c_{H2SO4} = 0/18.0$, where $\varepsilon_{329,1} = 5.66\times10^3$ M cm^{-1} and $\varepsilon_{291,1} = 3.87\times10^3$ M cm^{-1}. $\varepsilon_{329,obs,1-6}$ and $\varepsilon_{291,obs,1-6}$ are observed from UV-Vis absorption spectra of the six electrolytes compositions.

The optimization algorithm in MATLAB gave the results $\varepsilon_{329,2} = 2.56\times10^3$ M cm^{-1} and $\varepsilon_{291,2} = 6.60\times10^3$ M cm^{-1}. The molar composition of **1** and **2** can then be easily derived from the x values in different H_3PO_4-H_2SO_4 electrolytes based on stoichiometry. See optimized results and molar distribution of **1** and **2** in Table S1 and Fig. 2b.

Calculation of equilibrium constant (*K*c). The equilibrium constant (K_c) can be easily estimated based on the molar distribution, which is derived from UV-Vis spectra of 4×10^{-4} M vanadium(V) in H_3PO_4-H_2SO_4 electrolytes (Table S1).

First we consider an substitution equilibrium with constant reaction stoichiometry:

$$V_2{-}OSO_3H + n\ H_3PO_4 \rightleftharpoons V_2{-}OPO_3H_2 + n\ H_2SO_4$$

which involves the ligand substitution process of 1 equiv. of $V_2{-}OSO_3H$ dimer (**1**) by n equiv. of H_3PO_4 followed by the generation of 1 equiv. of $V_2{-}OPO_3H_2$ dimer (**2**) and n equiv. of H_2SO_4. The equilibrium constant (K_c) can thus be expressed as:

$$K_c = \frac{[\mathbf{2}]^1[\mathrm{H_2SO_4}]^n}{[\mathbf{1}]^1[\mathrm{H_3PO_4}]^n} = \frac{[\mathbf{2}]^1 c_{H2SO4}{}^n}{[\mathbf{1}]^1 c_{H3PO4}{}^n}$$

Then the following equation is obtained after transposition and logarithm of the formula above,

$$log_{10}\left(\frac{[\mathbf{1}]}{[\mathbf{2}]}\right) = -\,log_{10}(K_c) + n\;log_{10}\left(\frac{c_{H2SO4}}{c_{H3PO4}}\right)$$

which shows the linear relationship of the term $log_{10}\left(\frac{[1]}{[2]}\right)$ and the term $log_{10}\left(\frac{c_{H2SO4}}{c_{H3PO4}}\right)$. n and K_c can then be derived from the slope and intercept of the fitting curve (Fig. 2c), respectively. In this case, n = 1 and $K_c = 2.9$ at room temperature. Therefore, the proposed mechanism should be mono-substitution between V_2–OSO_3H dimer (**1**) and V_2–OPO_3H_2 dimer (**2**):

$$V_2\text{–}OSO_3H + H_3PO_4 \rightleftharpoons V_2\text{–}OPO_3H_2 + H_2SO_4$$

The mechanism of dimer-to-dimer transfer also fits in the fitting results of EAXFS (Table S2).

Data analysis of XAS results. X-ray absorption spectra (XAS), including X-ray absorption near edge spectra (XANES) and extended X-ray absorption fine structure (EXAFS), at V K-edge were collected in total-fluorescence-yield mode at ambient conditions at BL17C of National Synchrotron Radiation Center (NSRRC), Hsinchu, Taiwan. Given the difficulty in making accurate and precise XAFS measurements of very low concentration samples, the measurement with Cv = 10 mM was certainly possible to achieve a low noise level in spectra. Spectra were recorded in the energy range from −100 eV to 600 eV, relative to that of V K-edge absorption (5465.0 eV). The XAS spectra were processed by subtracting the baseline of pre-edge and normalizing that of post-edge. EXAFS analysis was carried out using Fourier transform on k^3-weighted EXAFS oscillations to assess the contribution of each bond pair to Fourier transform peak. The curve fitting of EXAFS spectra was conducted using the software, REX2000, with FEFF program.

Electrochemical characterization. Gamry Instruments Interface 1000E potentiostat was applied to process the electrochemical characterizations. All electrodes were purchased from CH Instruments, Inc., unless otherwise indicated. A three-electrode system was used in both cyclic voltammetry (CV) measurement and bulk electrolysis, in which Pt wire electrodes served as the counter electrode and pseudo-reference electrode. All potentials were reported with respect to the Hg_2SO_4/Hg (saturated K_2SO_4) electrode. The conversion between the reference electrode

(Hg_2SO_4/Hg) and the pseudo-reference electrode (Pt) followed the equation E(V vs. Hg_2SO_4/Hg) = E(V vs. Pt) + 0.755 V. The solution in electrochemical cell was saturated by continuous bubbling either CH_4 (Airgas, 99.5%) or N_2 (Airgas, 99.999%) with constant rates of 7.2 (CH_4) or 10 (N_2) standard cubic centimeters per minute (sccm), manipulated by a mass flow controller (Omega Engineering, Inc., FMA5510A). *i*R compensation was required during measurement.

Cyclic Voltammetry A 4 mL solution of 10 mM vanadium(V) in H_3PO_4-H_2SO_4 electrolytes was placed in a glass vial and saturated by bubbling N_2 or CH_4 for 20 mins with the assistance of stirring (150 rpm). CV data were recorded using a 2-mm Pt working electrode, a Pt wire pseudo-reference electrode, and a Pt wire counter electrode, covering different c_{H3PO4}/c_{H2SO4} and different scan rates (from 20 mV/s to 800 mV/s). The measured potentials were calibrated to Hg_2SO_4/Hg (saturated K_2SO_4) electrode based on open circuit potential (OCP) measurement. According to Randles-Sevcik equation, diffusion coefficient of vanadium species in different electrolytes were thus calculated from the peak current densities (j_p) shown in CV curves (Fig. S3 and S7).[4]

Bulk Electrolysis A 1 mL sample of the pre-electrolyzed solution was first reserved for following product analysis. A 4 mL solution of 10 mM vanadium(V) in H_3PO_4-H_2SO_4 electrolytes was electrolyzed at 2.25 V vs. Hg_2SO_4/Hg. The chronoamperometry was conducted for 6 h in a two-chamber setup with an FTO working electrode, a Pt wire pseudo-reference electrode, and a Pt wire counter electrode, meanwhile CH_4 (7.2 sccm) was bubbled into the solution with the assistance of stirring (150 rpm) (Fig. S5). Here the FTO working electrode was manufactured by connecting tungsten wire (0.01" diameter) to it and binding Teflon tapes so that the exposed surface area was 1 cm × 1 cm. After electrolysis, the functionalized products were analyzed by ^{1}H NMR spectroscopy, compared with the spectra of pre-electrolyzed solution (Fig. S6).

Product analysis. After 6 h product accumulation, quantitative ^{1}H NMR was conducted to analyze the products in liquid phase. The NMR sample was prepared by mixing a 0.4 mL aliquot of post-electrolyzed solution with 0.1 mL DMSO-d_6, in which acetic acid (AcOH) was used as the internal standard. A working curve was plotted by calibrating the linearity of the concentration of methyl bisulfate (MHS) and the its relative peak area with respect to AcOH. Here, chemical shift (δ) was expressed in parts per million (ppm). When using electrolytes of c_{H3PO4}/c_{H2SO4} = 0/18.0, a singlet peak at 3.34 ppm was assigned to MHS with two satellite peaks appearing either side of the main peak, whereas the singlet peak at 1.96 ppm was assigned to AcOH. If c_{H3PO4}/c_{H2SO4} increases, the product peak and the internal standard peak slightly shift to upfield due to change of bulk chemical environment. No liquid products other than MHS were observed in ^{1}H NMR spectra.

Determination of Faradaic efficiency (*FE*). To evaluate the selectivity of electrocatalyzed CH_4 functionalization, the Faradaic efficiency (*FE*) of bulk electrolysis was determined by the following relationship:

$$FE = \frac{nFc_{MHS}V_{electrolytes}}{Q_{overall}} \times 100\%$$

where F is the Faraday's constant (96485 C/mol), c_{MHS} is the concentration of MHS determined by ^{1}H-NMR, $V_{\mathrm{electrolytes}}$ is the volume of H_3PO_4-H_2SO_4 electrolytes used in bulk electrolysis, and the Q_{overall} is the total electric charges integrated from chronoamperometry. The constant n is the number of transferred electrons in electrochemical reaction when one equivalent of product is formed. In this case, n is 2 for the oxidation of CH_4 to MHS.

Calculation of apparent rate constant (k_{obs}). As mentioned before, the diffusion coefficient for vanadium complexes (D) is first calculated from the CV curves of different scan rates. The current density peak (j_{p}) under non-catalytic conditions is often used to account for D in freely-diffusing complexes with redox couples. D reflects the intrinsic physical property of vanadium(V)-oxo dimer in electrolytes. Data processing involves Randles-Sevcik equation[4]:

$$j_p = 0.4463 \times (nF)^{\frac{3}{2}} \times (RT)^{-\frac{1}{2}} \times C_{\mathrm{V}} \times (vD)^{\frac{1}{2}}$$

Here j_{p} is the peak current density of redox couple V(V)/V(IV), n is the number of electrons transferred in the redox event, F is the Faraday's constant, C_{V} is the total vanadium concentration, v is the scan rate, R is the gas constant, and T is the temperature of experiment.

The apparent rate constant (k_{obs}) of bulk electrolysis is calculated based on the following equation:

$$k_{obs} = (\frac{j_{CH4}}{nFC_{\mathrm{V}}})^2 D^{-1}$$

Here j_{CH4} is the partial current density of CH_4 oxidation in bulk electrolysis, n is the number of electrons required to generate one product molecule, F is the Faraday's constant, C_{V} is the total vanadium concentration, D is the diffusion coefficient of catalyst (for example, D is 10×10^{-8} $cm^2\cdot s^{-1}$ for vanadium species in the electrolyte of $c_{\mathrm{H3PO4}}/c_{\mathrm{H2SO4}} = 3.5/14.6$).

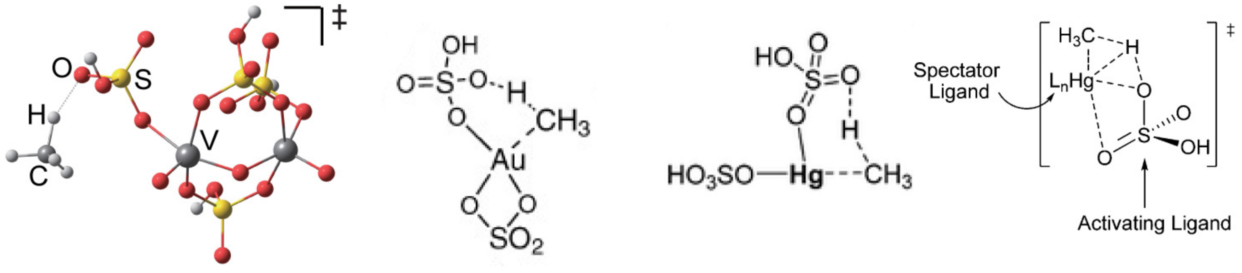

Nat. Commun. **2020,** *11* (1), 3686.

Angew. Chem. Int. Ed. **2004,** *43* (35), 4626-4629.

ACS Catal. **2016,** *6* (7), 4312-4322.

J. Mol. Struct.(Theochem) **1998,** *425* (1), 13-24.

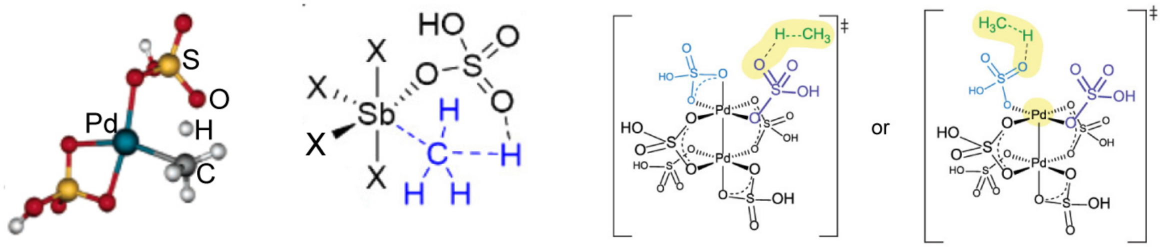

J. Am. Chem. Soc. **2006,** *128* (14), 4650-4657.

J. Am. Chem. Soc. **2021,** *143* (43), 18242-18250.

ACS Catal. **2020,** *10* (24), 14782-14792.

Fig. S1 Reported transition states of metal-catalyzed C–H activation in H_2SO_4 (stuctures mentioned in the main text).

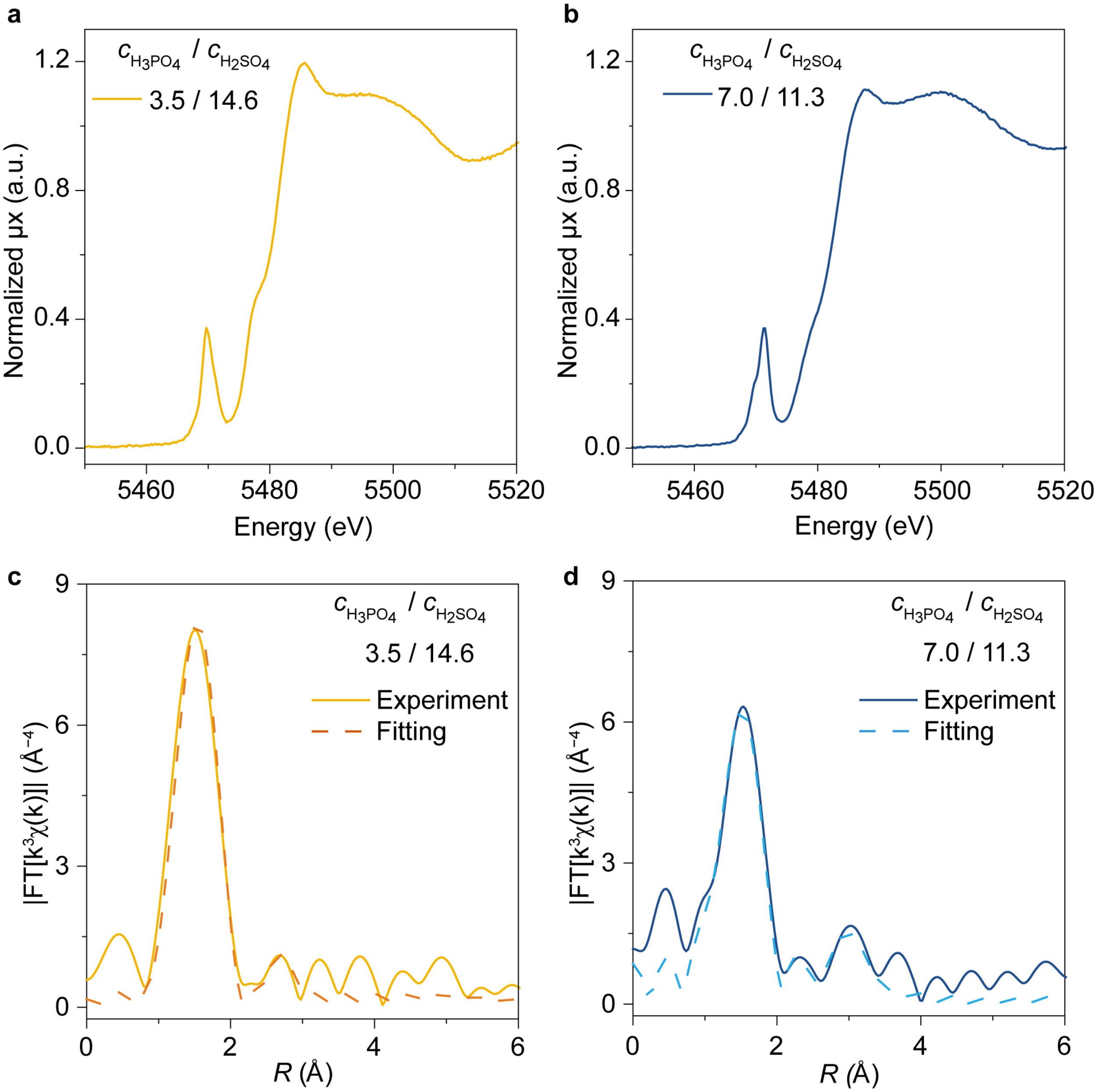

Fig. S2 X-ray absorption spectra (XAS) results for vanadium species. a, **b**, K-edge X-ray absorption near-edge structure (XANES) spectra data for C_v = 10 mM in H_3PO_4-H_2SO_4 electrolytes of c_{H3PO4} / c_{H2SO4} = 3.5/14.6 (**a**) and 7.0/11.3 (**b**). **c**, **d**, Extended X-ray absorption fine structure (EXAFS) *R*-space curves for the experimental and fitting results of C_v = 10 mM in H_3PO_4-H_2SO_4 electrolytes of c_{H3PO4} / c_{H2SO4} = 3.5/14.6 (**c**) and 7.0/11.3 (**d**).

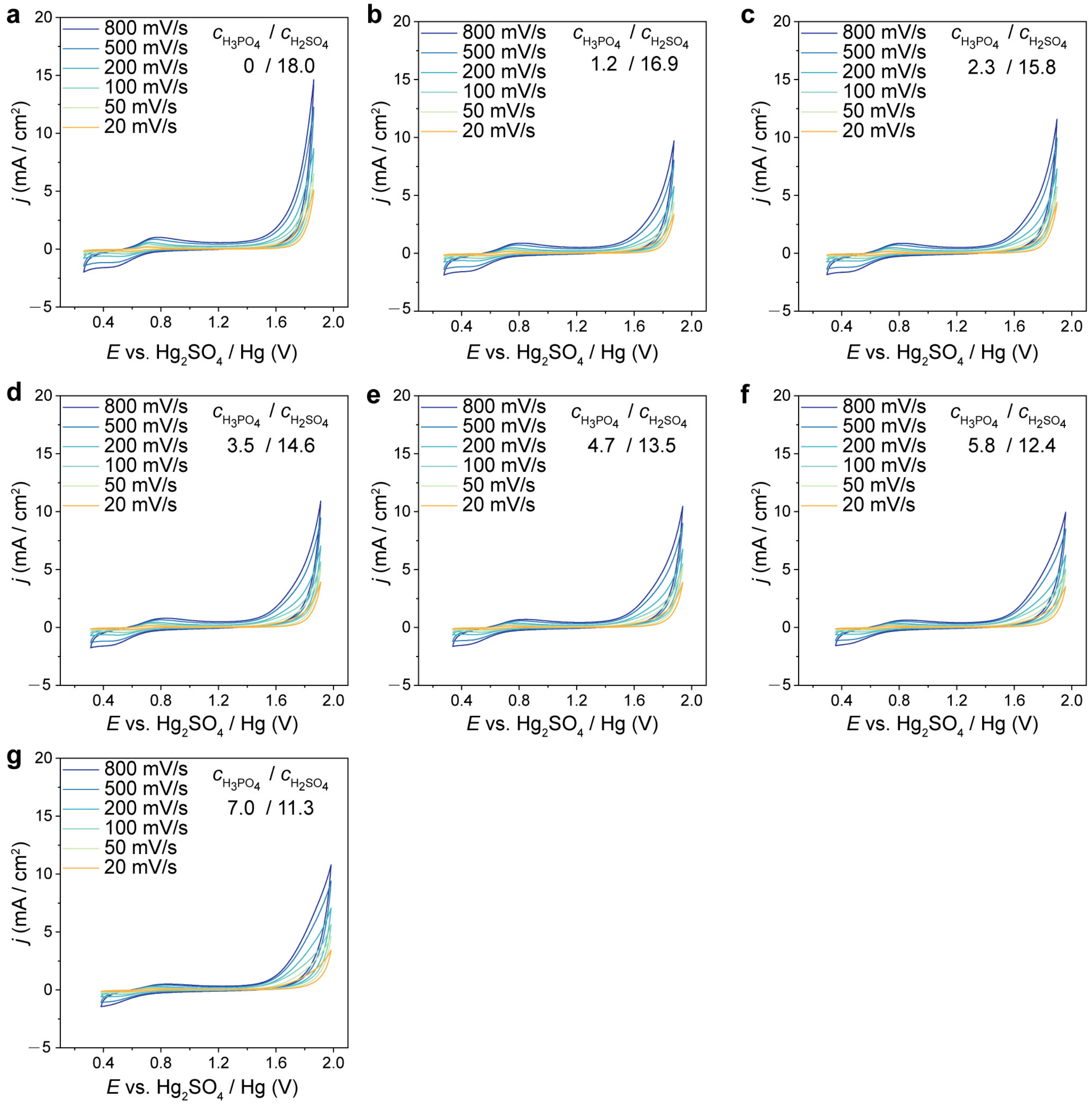

Fig. S3 Cyclic voltammograms of vanadium(V) saturated in N_2 with various scan rates (from 20 mV·s^{-1} to 800 mV·s^{-1}) in H_3PO_4-H_2SO_4 electrolytes of different compositions. c_{H3PO4}/c_{H2SO4} = 0/18.0 (**a**), 1.2/16.9 (**b**), 2.3/15.8 (**c**), 3.5/14.6 (**d**), 4.7/13.5 (**e**), 5.8/12.4 (**f**), and 7.0/11.3 (**g**). C_v = 10 mM, 2 mm diameter Pt electrode as working electrode.

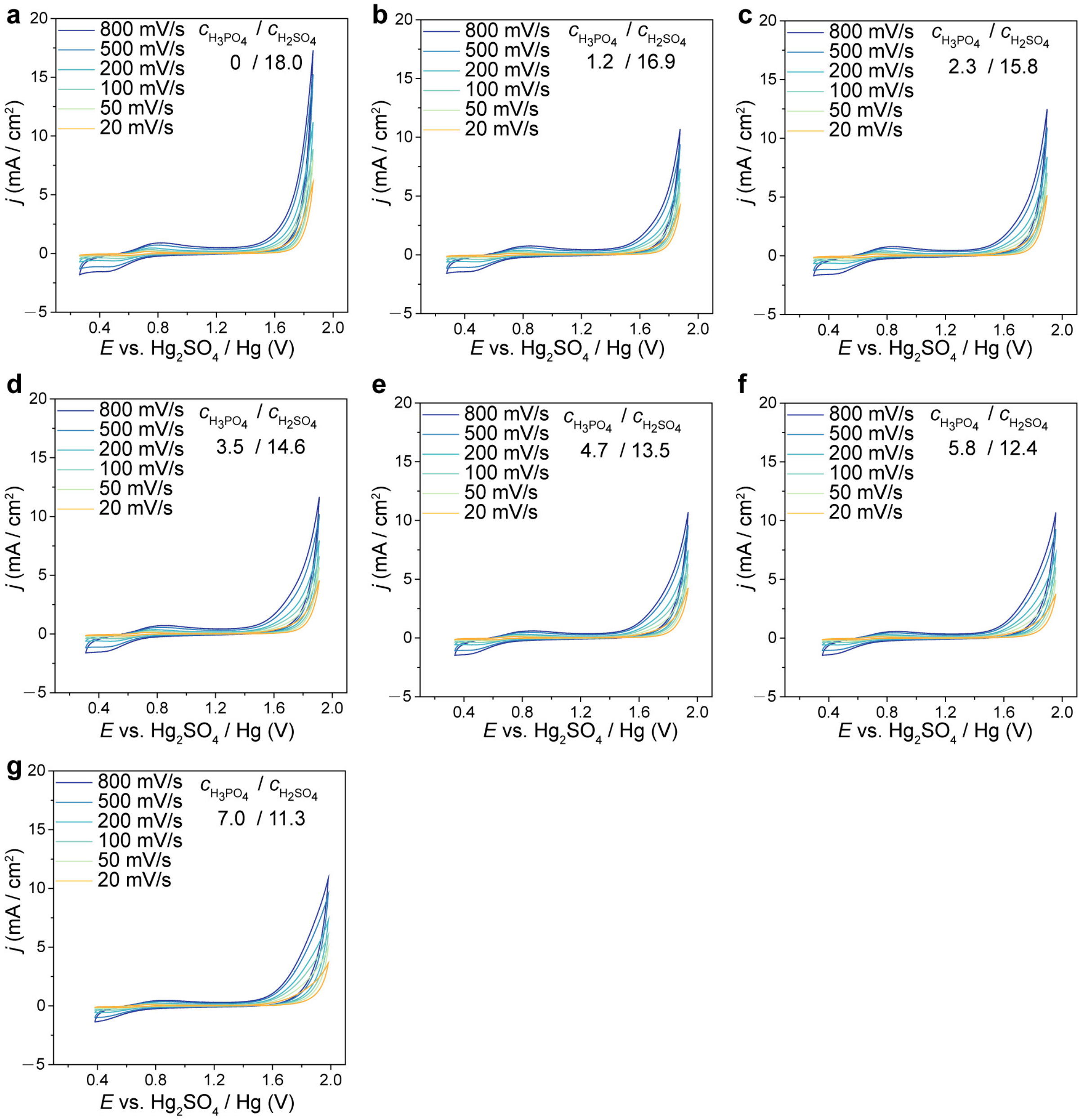

Fig. S4 Cyclic voltammograms of vanadium(V) saturated in CH_4 with various scan rates (from 20 mV·s^{-1} to 800 mV·s^{-1}) in H_3PO_4-H_2SO_4 electrolytes of different compositions. c_{H3PO4}/c_{H2SO4} = 0/18.0 (**a**), 1.2/16.9 (**b**), 2.3/15.8 (**c**), 3.5/14.6 (**d**), 4.7/13.5 (**e**), 5.8/12.4 (**f**), and 7.0/11.3 (**g**). C_v = 10 mM, 2 mm diameter Pt electrode as working electrode.

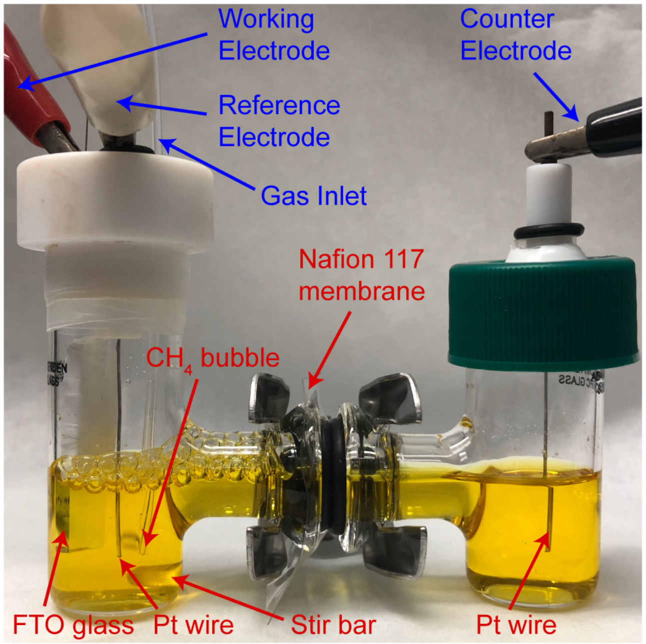

Fig. S5 A schematic illustration of two-chamber setup for bulk electrolysis in CH_4. Such electrolysis is conducted at room temperature for 6 h with an FTO working electrode, a Pt wire pseudo-reference electrode, and a Pt wire counter electrode, meanwhile CH_4 (7.2 sccm) is bubbled into the solution with the assistance of stirring (150 rpm).

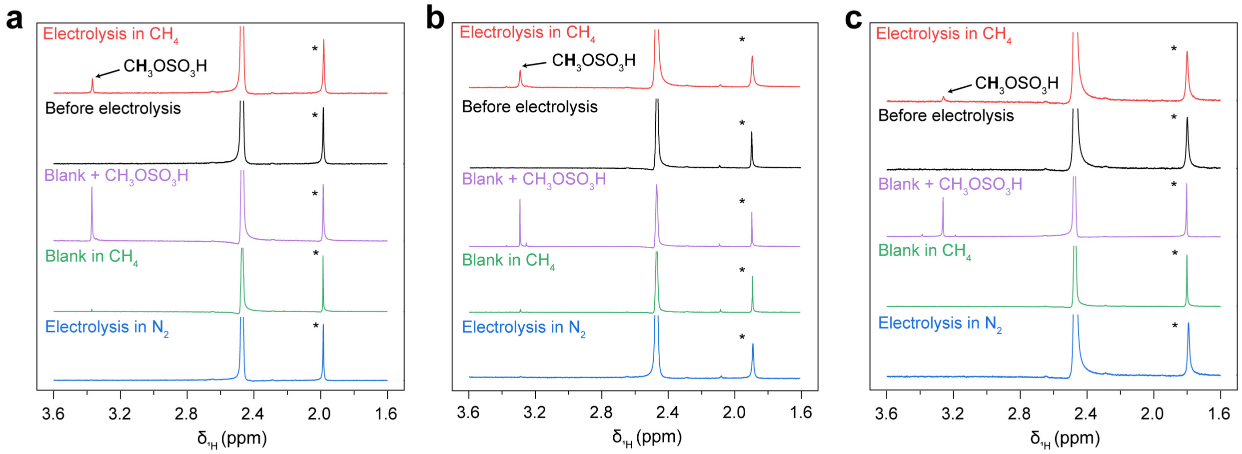

Fig. S6 Product analysis of 6 h bulk electrolysis in H_3PO_4-H_2SO_4 electrolytes. c_{H3PO4}/c_{H2SO4} = 0/18.0 in **a**, 3.5/14.6 in **b**, and 7.0/11.3 in **c**. ^{1}H NMR spectra for vanadium(V) solution (C_v = 10 mM) before (black) and after (red) electrolysis in CH_4, CH_3OSO_3H standard substance in blank solution without vanadium(V) (purple), blank solution after electrolysis in CH_4 (green), vanadium(V) solution (C_v = 10 mM) after electrolysis in N_2 (blue). *, Acetic acid as internal standard. All electrolysis experiments were conducted at E = 2.25 V vs. Hg_2SO_4/Hg. Notice that the quantitative comparison among the panels is not applicable here due to the different calibration curves prepared in each panel.

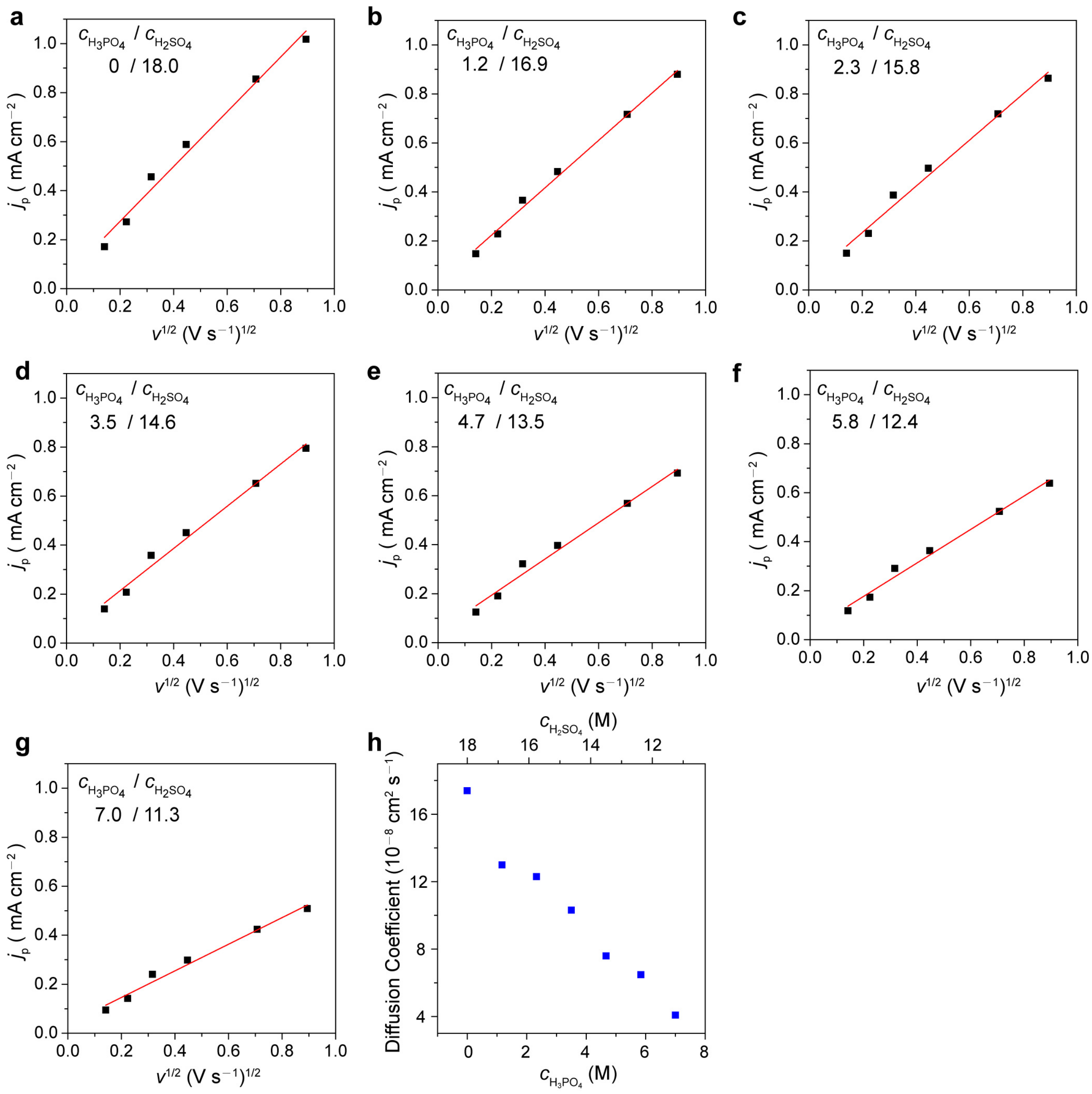

Fig. S7 Derivation of diffusion coefficients of vanadium(V) in H_3PO_4-H_2SO_4 electrolytes. Linear fitting of anodic peak current density (j_p) versus the square root of scan rates ($v^{1/2}$) (raw data shown in Fig. S2) in electrolytes of c_{H3PO4}/c_{H2SO4} = 0/18.0 (**a**), 1.2/16.9 (**b**), 2.3/15.8 (**c**), 3.5/14.6 (**d**), 4.7/13.5 (**e**), 5.8/12.4 (**f**), and 7.0/11.3 (**g**). **h**, Change of diffusion coefficients D in different electrolytes compositions derived by the slopes of **a** to **g** with Randles-Sevcik equation (see Table S3 for exact data).

Table S1. The optimized molar distribution of 1 and 2 solved by MATLAB.

c_{H3PO4}/c_{H2SO4} (M/M)	Atomic percentage of vanadium in **1**, x (%)	Atomic percentage of vanadium in **2**, $1{-}x$ (%)	Considering **2** is a vanadium dimer	
			Molar composition of **1**, [**1**]/([**1**]+[**2**]) (%)	Molar composition of **2**, [**2**]/([**1**]+[**2**]) (%)
0/18.0	100	0	100	0
1.2/16.9	88	12	88	12
2.3/15.8	77	23	77	23
3.5/14.6	67	33	67	33
4.7/13.5	56	44	56	44
5.8/12.4	46	54	46	54
7.0/11.3	35	65	35	65

Table S2. Comparison of structural information between UV-Vis spectroscopy and fitted EXAFS results.

Method	Considering **2** is a vanadium dimer	For c_{H3PO4}/c_{H2SO4} = 3.5/14.6	For c_{H3PO4}/c_{H2SO4} = 7.0/11.3
UV-Vis	[**1**]/[**2**] [a]	67.2/32.8	35.1/64.9
	Expected C.N.$_{V–S}$/C.N.$_{V–P}$ [b]	84/16	68/32
EXAFS	Fitted C.N.$_{V–S}$/C.N.$_{V–P}$ [c]	8/2	6/4

[a] [**1**]/[**2**], molar ratio of **1** and **2** derived from the corresponding molar composition measured by UV-Vis spectroscopy (see Fig. 2b and Table S1).

[b] C.N., coordination number; C.N.$_{V–S}$/C.N.$_{V–P}$, coordination number ratio of shell V−S (non-bridging –OSO_3H ligand) and V−P (non-bridging –OPO_3H_2 ligand) derived from the molar ratio [**1**]/[**2**].

[c] C.N.$_{V–S}$/C.N.$_{V–P}$ fitted from experimental EXAFS data, which were recorded for C_v = 10 mM in H_3PO_4-H_2SO_4 electrolytes of either c_{H3PO4}/c_{H2SO4} = 3.5/14.6 or c_{H3PO4}/c_{H2SO4} = 7.0/11.3.

Table S3. Diffusion coefficients of vanadium(V) in H_3PO_4-H_2SO_4 electrolytes.

c_{H3PO4}/c_{H2SO4} (M/M)	D ($\times 10^{-8}$ cm^2 s^{-1}) [a]
0/18.0	17
1.2/16.9	13
2.3/15.8	12
3.5/14.6	10
4.7/13.5	7.6
5.8/12.4	6.5
7.0/11.3	4.1

[a] Exacted from Randles-Ševčík analysis under non-catalytic conditions (Fig. S7).

Supplementary Notes

Part 1: Choice of H_3PO_4

We considered H_3PO_4 as a safe choice compared to other inorganic acids, HNO_3 and HCl. While there is no direct evidence that H_3PO_4 is more inert than H_2SO_4, some facts of their chemical properties indicate that H_3PO_4 is harder to be anodically oxidized than H_2SO_4. Reasonable comparisons can be made based on their oxidized forms, i.e., peroxo species. 1) The peroxodiphosphate anion ($P_2O_8^{4-}$) is a stronger oxidizing agent with an oxidation potential of 2.07 V, whereas the peroxydisulfate ($S_2O_8^{2-}$) anion has a lower oxidation potential of 2.01 V.[5] 2) Peroxodiphosphoric acid ($H_4P_2O_8$) could be prepared by anodic oxidation of H_3PO_4 but $H_4P_2O_8$ is rare to find in nature and cannot be produced commercially; peroxodisulfuric acid ($H_2S_2O_8$) is more common and can be manufactured by anodic oxidation of sulfuric acid in industry.[6]

Part 2: Causation of the decreasing activities with the increase of c_{H3PO4} / c_{H2SO4}

The electrochemical accessibility of the cation radical $V_2^{V,V\bullet+}$ mostly localized on the monodentate bisulfate ligand. With the increase of c_{H3PO4} / c_{H2SO4} value, the molar composition of **1** decreases and **2** is becoming the predominant species accompanied by the decrease of the number of redox active sites on bisulfate ligand, which leads to a decreased value of averaged activities (k_{obs} in Fig. 3g in main text).

Additional References

1. Deng, J.; Lin, S.-C.; Fuller, J.; Iñiguez, J. A.; Xiang, D.; Yang, D.; Chan, G.; Chen, H. M.; Alexandrova, A. N.; Liu, C. Ambient Methane Functionalization Initiated by Electrochemical Oxidation of a Vanadium (V)-oxo Dimer. *Nat. Commun.* **2020**, *11*, 3686.
2. Braslavsky, S. E. Glossary of Terms Used in Photochemistry, 3rd ed. (IUPAC Recommendations 2006). *Pure Appl. Chem.* **2007**, *79*, 293-465.
3. Cohen, M. D.; Fischer, E. 588. Isosbestic points. *J. Chem. Soc.* **1962**, 3044-3052.
4. Zanello, P.; Nervi, C.; de Biani, F. F. *Inorganic Electrochemistry: Theory, Practice and Application*; RSC: Cambridge, UK, 2003.
5. Groenen Serrano, K. A Critical Review on the Electrochemical Production and Use of Peroxo-compounds. *Curr. Opin. Electrochem.* **2021,** *27*, 100679.

6 Jakob, H.; Leininger, S.; Lehmann, T.; Jacobi, S.; Gutewort, S. Peroxo Compounds, Inorganic. In *Ullmann's Encyclopedia of Industrial Chemistry*; Wiley-VCH: Weinheim, 2007.